

Electrochemical performance of ternary s-GN/PANI/CNTs nanocomposite as supercapacitor power electrodes

Muhammad Al-badri¹, Mushtaq Albdiry²

¹Department of Chemical Engineering, University of Al-Qadisiyah

²Department of Materials Engineering, University of Al-Qadisiyah

ABSTRACT

In this paper, binary carbon nanotubes (CNTs) reinforced conducting polyaniline (PANI) and ternary sulfonated Graphene nanosheets (s-GN) decorated CNT@PANI nanocomposites were prepared using a solution mixing followed by ultrasonic dispersion. The SEM and XRD analysis found that the s-GN and CNTs have uniformly sandwiched the PANI. The cyclic voltammetry (CV) results showed that the sulfonated graphene along with CNTs have led to increase the electrochemical capacitance from 305 F/g for the binary CNT₂₀@PANI to 419 F/g for the ternary CNT₂₀@PANI@s-GN₂₀ nanocomposites (37 % increase). This increase is attributed to the free mobility of the electronic carriers on the s-GN surface for the larger surface area and presence of the SO⁻³ groups. The electrochemical impedance spectroscopy (EIS) measurements exhibited that the s-GN embedded PANI@CNT nanocomposite resulted in a higher energy density of 209 Wh/kg with a power density of 381 W/kg at scan rate of 5 mV/s in an electrolyte of 0.5M H₂SO₄. The prepared s-GN@PANI@CNTs nanocomposites are promising electrode's materials for the electrochemical capacitors power systems.

Keywords: Polyaniline, Graphene, CNT/PANI, electrochemical, cyclic voltammetry

Corresponding Author:

Muhammad Al-badri
Department of Chemical Engineering
University of Al-Qadisiyah
Al-Qadisiyah, Iraq
eng.mohammed.abdalrodhal@qu.edu.iq

1. Introduction

The global warming concerns due to the CO₂ emissions from the fossil fuel and the energy depletion highly encourage the researchers to emphasize their efforts on alternative clean and renewable energy storage (or conversion) sources [1]. Examples on these sources are fuel cells, batteries and supercapacitors. The supercapacitors consider as an electrical storage technology enormously used for aerospace, electrical vehicles, electronic devices, and emergency power systems for their good charging/discharging ability and cyclic stability [2]. The supercapacitors have a good power density, a stable cycle life but lower energy density (or specific capacity) when compared to the Li-batteries. Polyaniline (PANI) as conducting material has been broadly used as capacitors' electrodes since it is easy to prepare, chemical stable, and good electrons affinity [3]. However, PANI undergoes structural deformation and poor capacitance performance due to the continuous electrochemical process of energy conversion (or energy storage). The structural and electrochemical properties of PANI and thereby the specific capacity and performance of the capacitors' electrodes can be enhanced without sacrificing the high-power density by incorporating various nanomaterials like graphene nanosheets (GNs) or reduced graphene oxide (rGO) and carbon nanotubes (CNTs) [4], [5]. The electrochemical performance based on the cyclic voltammetry (CV) test of a binary rGO/PANI composite's electrode exhibited a good capacitance due to the capacitive of PANI and the conductivity of rGO [6]. The electrochemical performance has also improved with higher specific capacitance when the electrode's material, rGO_{6.7%}/PANI_{93.33%} doped with methane sulphonic acid. Effect of dopant has resulted in higher energy storage at higher numbers of charge/discharge cycles [7].

A ternary graphite/PANI/CNTs composite's electrode has conducted a higher specific capacitance and better energy/power performance for the increased surface area of electroactive and decreased constriction/spreading resistance compared to the binary PANI/CNTs electrodes [8]. Preparation of a ternary CuO_{13%}/rGO_{7%}/PANI_{80%} nanocomposite as electrode's material exhibited a good specific capacitance and perfect specific energy and power properties owing to the integration of rGO/PANI/CuO. In the current study, the electrochemical

properties of a novel ternary sulfonated graphene nanosheets (GNs) uniformly wrapped PANI/CNTs nanocomposites have been measured according to the obtained CV and EIS analysis. The role of sulfonic acid as dopant material for the ternary s-GN/PANI/CNTs nanocomposite on the structural characteristics, specific faradaic capacitance, and electrochemical stability has been comprehensively discussed.

2. Experimental

2.1. Materials used

Graphene nanopowders (GN) of 7 nm thickness and 99.7% purity obtained from Skyspring Nanomaterials, USA, and multiwalled carbon nanotubes (MWCNTs) having an average length of 22 nm, OD of 20 nm, and ID of 8 nm obtained from Cheap Tubes, USA were used. Water-dispersible polyaniline (PANI) of 25 nm nanoparticles obtained from Panichem Co. Ltd, South Korea. The chemical used were, sulphuric acid (H₂SO₄) of 98%, laboratory reagent (Thomas Baker) and extra pure hydrochloric acid (HCl) of 37% was obtained from Scharlau.

2.2. Nanocomposites preparation

A binary CNTs_{20%}/PANI_{80%} nanocomposite was prepared using in-situ direct chemical mixing of 2 g of PANI particles sonicated in 1 M HCl (40 mg ml⁻¹) for 30 min at 25 °C, and 400 mg of CNTs sonicated in 1 M HCl (2 mg ml⁻¹) for 30 min at 25 °C, on a magnetic stirrer for 30 min at 50 °C. The same procedure was repeated for the preparation of a ternary s-GN_{20%}/CNTs_{20%}/PANI_{60%} nanocomposite, with 400 mg of GN sonicated in 1M HCl (2 mg ml⁻¹) for 30 min at 25 °C, mixed with 20 ml methanol and 20 ml 0.5M H₂SO₄ solution using ultrasonication for 30 min at 40°C. The obtained s-GN powders were incorporated with CNTs/PANI on a hot magnetic stirrer for 30 min at 50 °C. The resultant mixture was dewatered by ultrafiltration and rinsed by water to reach pH of 7, and thereby dried at 90 °C for 2 h. The dried s-GN_{20%}/CNTs_{20%}/PANI_{60%} powders were collected for further determination of the characteristic.

2.3. Structural characteristics

The crystalline structures of the CNT/PANI and CNT/PANI/s-GN nanocomposites were conducted using X-ray diffraction (XRD) by Lab X, XRD-6000 (Shimadzu, Japan) with CuK α radiation of 1.54 Å. The XRD patterns were collected based on 0.05° step at a step time of 5°/min and preset time 0.6 sec over a range of 10° ≤ 2 θ ≤ 60°. The morphological properties and particles dispersion of both materials were examined using the scanning electron microscopy (SEM).

2.4. Capacitance measurement

The capacitance of all electrodes was measured based on the cyclic voltammetry (CV) and electrochemical impedance spectroscopy (EIS) in 0.5 M H₂SO₄ electrolyte using three electrode potentiostat/galvanostat system including reference Ag/AgCl electrode, Pt as the counter and glassy carbon (GC) as working electrode. The CV test was carried out at potential values from -0.2 to 0.8 V and scan rates ranging from 1 to 50 mV/s. The EIS tests at AC voltage of 5 mV amplitude and frequency (1Hz - 20 kHz) were employed based on the open circuit potential (OCP) and digital mode. The supercapacitor electrodes of 4 mg active material (CNTs/PANI or s-GN/PANI/CNTs composites) were prepared by drop casting. The powdery active materials were homogeneously sonicated in deionized water for 10 minutes, and 2 μ l of which was casted on a 2 mm diameter GCE and then dried overnight at ambient temperature.

The specific gravimetric capacitances of all samples were determined applying the equation [2]:

$$C_s = \frac{\int_{V_{min}}^{V_{max}} I(V)dv}{2mv(V_{max}-V_{min})} \dots (1)$$

where C_s is the specific capacitance in F/g, I is the discharge current in (A), $V_{max} - V_{min}$ is the potential (V), m is mass of electroactive on the electrode (mg), $\int_{V_{min}}^{V_{max}} I(V)dv$ is the area of CV curve, and v is the scan rate. The factor 2 indicates that only half of the area in the CV curve is associated with the total charge stored.

The specific energy (S.E) measured in Wh/kg and the specific power (S.P) measured in W/kg of the electrodes were determined using the following equations [6]:

$$Specific\ Energy\ (S.E) = \frac{C_s \times (\Delta V)^2}{2} \dots (2)$$

$$Specific\ Power\ (S.P) = \frac{S.E}{\Delta t} \dots (3)$$

3. Results and discussion

3.1. SEM analysis

SEM images of the binary CNT₂₀/PANI and the ternary CNT₂₀/PANI/s-GN₂₀ nanocomposites are depicted in Figure 1. Effects of graphene surface treatment have clearly manifested in a homogenous dispersion of s-GN powders on the meshed (porous) surface of the CNTs/PANI composite. The sulfonated s-GN surface Fig. 1b also manifested in a spherical dense structure that is in turn resulted in a higher surface area and shorter path of ion mobility [9]. The CNTs/PANI structure, Figure 1a, however shows a flake-like structure despite the PANI particles uniformly distributed on the MWCNTs structure, and similarly such a structure has been confirmed in [10].

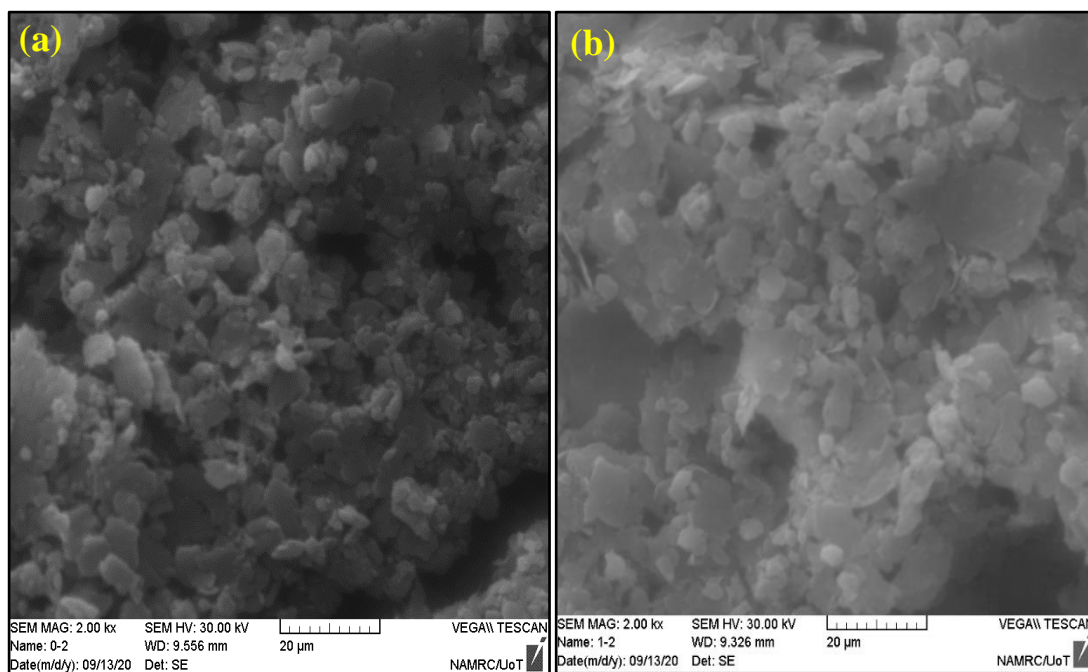


Figure 1. SEM images for (a) CNT₂₀/PANI₈₀; & (b) CNT₂₀/PANI₆₀/s-GN₂₀ nanocomposites

3.2. XRD Analysis

The XRD patterns for the CNT₂₀/PANI₈₀, and the CNT₂₀/PANI₆₀/GN₂₀ nanocomposites powders are illustrated in Figure 2. The XRD peaks of both the binary MWCNTs/PANI and the ternary MWCNTs/PANI/s-GN nanocomposites depict two sharp intensities at 25.75° and 43.93°, indicating the (002) plane for the MWCNTs. The peak at 25.4° in Fig. 2b is referring for the increase in the interlayer distance of the s-GN sheets due to the intercalation among their functional groups [11]. The XRD peak at 2θ = 54.7° in the CNTs/PANI/s-GN nanocomposite could be ascribed to the effect of SO⁻³ functional group on the sulfonated s-GN nanopowders' surface [12].

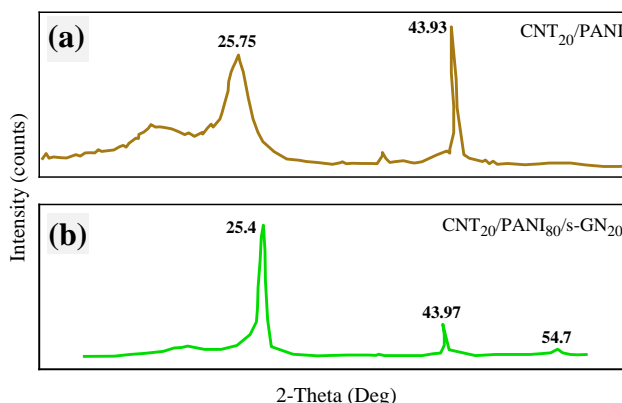


Figure 2. XRD patterns of the CNT₂₀/PANI; & the CNT₂₀/PANI/s-GN₂₀ nanopowders

3.3. Capacitance performance

The specific capacitances of the binary CNT₂₀/PANI₈₀ and ternary CNT₂₀/PANI₈₀/s-GN₂₀ nanocomposites' electrodes were measured based on the electrochemical CV tests. The CV curves of the binary and ternary nanocomposites in a potential (-0.2 to 0.8 V) at scan rates (1, 5, 10, 30 and 50 mV/s) using three electrodes system with 0.5 M H₂SO₄ as electrolyte are shown in Figures 3 and 4, respectively.

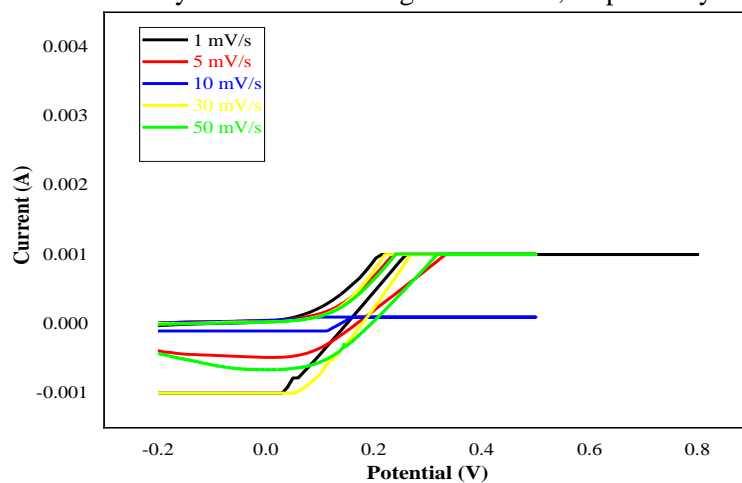


Figure 3. The CV curves for the binary CNTs₂₀/PANI₈₀ nanocomposites at different scan rates

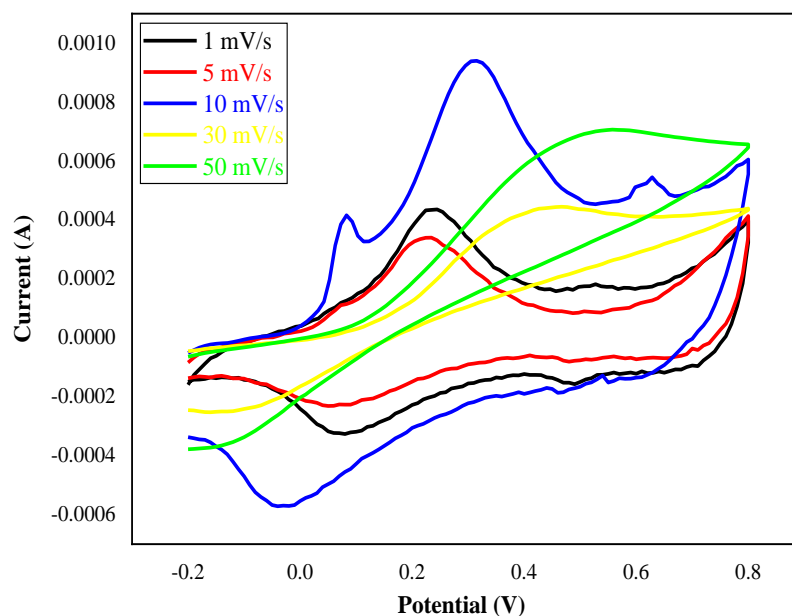


Figure 4. The CV curves for the ternary CNT₂₀/PANI₆₀/s-GN₂₀ nanocomposites at different scan rates

According to Eq.1, values of the electrochemical capacitances are directly dependent on the area of the CV curve. From Figure 4, it can be clearly noticed that at the same scan rates, areas of the CV curves for the ternary composite are larger than those for the binary composite's electrodes (Figure 3), resulting in a higher specific capacitance. The CV curves of the ternary electrodes are quasi rectangular, indicating the typical electrochemical capacitive behavior [2]. Interestingly, all CV curves of the ternary electrodes had two pair of redox (anodic and cathodic) peaks that is indicating the occurrence of the capacitance between the electrode and the electrolyte surface [6]. The first pair refers to the redox of PANI between a semiconducting and a conducting state, and the second pair refers to the transformation between the benzo-quinone and hydro-quinone pair for the cross-linking reaction of PANI chains [13]. However, these redox peaks are being relatively lower in the CVs of the binary electrodes, resulting in lower current densities as can be observed in Figure 3. This could be attributed to the discharge from the binary electrode surface during cycling [7]. The CV curves of the binary CNT/PANI electrode imply steady current densities of 1 mA/g associating with the increases in the potential

scan rates, indicating that the material had a limited anodic and cathodic reaction, and consequently a limited faradic process and poor Pseudo-capacitor. Importantly, areas of the CV curves of the ternary s-GN/PANI/CNTs electrodes do not significantly change with increasing of the scan rates (see Figure 4). This means that the redox reactions are symmetry which manifest a higher power properties and satisfactory cycling stability. The specific capacitance (C_s) was measured applying value of the steady charging/discharging cycle of 5 mV/s scan rate. The C_s value for the binary CNTs/PANI has improved by 37 % from 305 F/g to 419 F/g with the incorporation of sulfonated Graphene nanopowders (s-GN) at 5 mV/s scan rate and 0.5 M H_2SO_4 electrolyte. The sulfonated Graphene works to increase the surface area, restrict the diffusion ions from the electrolyte to the electrode, and maintain a good pseudo-capacitor store. Meanwhile, the specific capacitances for all materials have obviously declined during cycles at higher rates, 30 mV/s or 50 mV/s. The electrochemical capacitive characteristics of CNT/PANI and s-GN/PANI/CNTs electrodes, Figures 5a and b describes the GCD tests of these electrodes at 10 mA/g current density. The s-GN/PANI/CNTs composite electrode (Figure 5b) had the longest discharge time and the lowest impedance, which is important for capacitors, since this manifest in a lower production of unwanted heat during the cycling process.

The highest specific energy and the specific power for the ternary s-GN/PANI/CNTs electrode-based supercapacitor are 209.6 Wh/kg and 381 W/kg; 152.3 Wh/kg and 339 W/kg for the binary PANI/CNTs electrode, respectively.

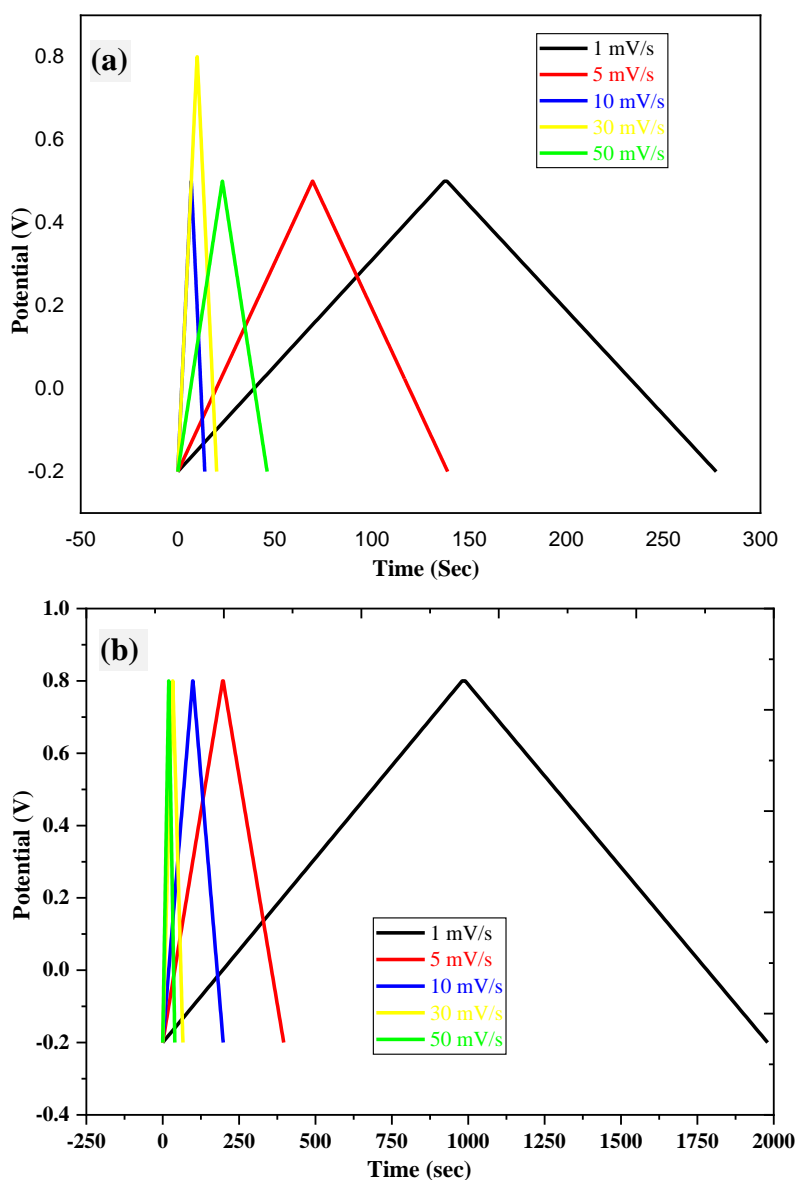


Figure 5. GCD curves of (a) binary CNT/PANI; and (b) ternary s-GN/PANI/CNTs electrodes at different scan rates.

4. Conclusions

The structural characteristics and the electrochemical performance of the binary CNT₂₀/PANI and the ternary s-GN₂₀/PANI/CNT₂₀ nanocomposites' electrodes-based supercapacitors have been investigated. The role of sulfonated s-GN nanopowders on the specific capacitances and power densities have been identified. The s-GN nanopowders have uniformly wrapped the CNTs/PANI, resulted in a dense and spherical microstructure. The ternary electrode had the longest discharge time and the highest specific capacitance and energy/power densities of 419 F/g, 209.6 Wh/Kg and 381 W/Kg versus 305 F/g, 152.3 Wh/Kg and 339 W/Kg for binary CNT/PANI electrode, respectively. The enhancements in electrochemical properties can be ascribed to the increased surface area and the enhanced charge carriers of the electron due to the sulfonated graphene. The prepared ternary nanocomposite's electrode can be effectively considered as good promise for the highly efficient supercapacitor.

References

- [1] P. Mitta. "Molecular Design of Solid-State Nanopores: Fundamental Concepts and Applications." *Advanced Materials* 31.37 (2019): 1901483.
- [2] A. Viswanathan and A. Shetty, "Facile in-situ single step chemical synthesis of reduced graphene oxide-copper oxide-polyaniline nanocomposite and its electrochemical performance for supercapacitor application," *Electrochimica Acta*, vol. 257, pp. 483–493, 2017.
- [3] A. Ibtisam A, A. Huda, A. H. Alrikabi, "Simulation Study to Calculate the Vibration Energy of Two Molecules of Hydrogen Chloride and Carbon Oxide," *Journal of Green Engineering*, vol. 10, no. 9, pp. 5989-6010, 2020.
- [4] A. Balducci, D. Belanger, T. Brousse, J. W. Long, and W. Sugimoto, "A Guideline for Reporting Performance Metrics with Electrochemical Capacitors: From Electrode Materials to Full Devices," *Journal of The Electrochemical Society*, vol. 164, no. 7, 2017.
- [5] K. Dimitrios, E. Banks, "A new approach for the improved interpretation of capacitance measurements for materials utilised in energy storage," *RSC Adv.*, no. 5, pp. 12782–12791, 2015.
- [6] M. Shabani-Nooshabadi and F. Zahedi, "Electrochemical reduced graphene oxide-polyaniline as effective nanocomposite film for high-performance supercapacitor applications.," *Electrochimica Acta*, vol. 245, pp. 575–586, 2017.
- [7] A. Viswanathan and A. N. Shetty, "Effect of dopants on the energy storage performance of reduced graphene oxide/polyaniline nanocomposite.," *Electrochimica Acta*, vol. 327, p. 135026, 2019.
- [8] H. Zhou, X. Zhi, and H. Zhai, "A facile approach to improve the electrochemical properties of polyaniline-carbon nanotube composite electrodes for highly flexible solid-state supercapacitors," *International journal of hydrogen energy*, vol. 43, pp. 18339–18348, 2018.
- [9] O. A. Al-Hartomy, S. Khasim, A. Roy, and A. Pasha, "Highly conductive polyaniline/graphene nanoplatelet composite sensor towards detection of toluene and benzene gases," *Applied Physics A*, vol. 125, no. 12, Art. no. 12, 2019.
- [10] Z. Wu, S. Zhu, and X. Dong, "A facile method to graphene oxide/polyaniline nanocomposite with sandwich-like structure for enhanced electrical properties of humidity detection," *Analytica Chimica Acta*, vol. 1080, pp. 178–188, 2019, doi: <https://doi.org/10.1016/j.aca.2019.07.021>.
- [11] R. Li, H. Xu, and R. Fu, "Preparation of 3D reduced graphene oxide/carbon nanospheres/polyaniline ternary nanocomposites as supercapacitor electrode," *Reactive and Functional Polymers*, vol. 125, pp. 101–107, 2018.
- [12] L. Zhang, D. Huang, and N. Hu, "Three-dimensional structures of graphene/polyaniline hybrid films constructed by steamed water for high-performance supercapacitors," *Journal of Power Sources*, vol. 342, pp. 1–8, 2017.
- [13] X. Lu, H. Dou, and S. Yang, "Fabrication and electrochemical capacitance of hierarchical graphene/polyaniline/carbon nanotube ternary composite film.," *Electrochimica Acta*, vol. 56, pp. 9224–9232, 2011.